

# EFFECT OF GRAPHENE OXIDE AQUEOUS DISPERSIONS ON ROCK WETTABILITY

## EFECTO DE LAS DISPERSIONES ACUOSAS DE ÓXIDO DE GRAFENO SOBRE LA HUMECTABILIDAD DE LAS ROCAS

José Carlos Cárdenas<sup>1\*</sup>, Angelli Stephanie Pérez<sup>1</sup>, Rodrigo Torres Saez<sup>1</sup>,  
Emiliano Ariza León<sup>2</sup>

<sup>1</sup>Instituto Colombiano del Petróleo-ICP, Ecopetrol.

<sup>2</sup>Universidad Industrial de Santander, Colombia.

Email: jose.cardenasmo@ecopetrol.com.co\*, angepeca90@gmail.com,  
rodrigo.torres@ecopetrol.com.co, earizal@uis.edu.co

Recibido: 28 de julio, 2023. Aprobado: 31 de julio, 2023. Versión final: 22 de enero, 2024

### Abstract


Among the various methods to improve oil recovery from reservoirs (wells stimulation), the use of nanofluids has emerged as a promising alternative for modifying the wettability and permeability of sandstone rocks. For this reason, in this study, graphene oxide (GO) was synthesized from graphite, and a nanofluid was formulated using GO dispersed in water to evaluate its capacity for modifying wettability on sandstone core plugs from Colombian reservoirs. The experimental setup included three preliminary tests: visual wettability, contact angle measurements, and detergency. The results demonstrated an increase in the water wettability of the rocks, leading to a decrease in the contact angle of the water-rock system by up to 42.6%. Additionally, the visual wettability and detergency tests yielded positive results, indicating that graphene oxide is an effective wettability modifier, rendering the rock more water-wet.

**Keywords:** Permeability Modifier, Rock Wettability, Graphene Oxide.

### Resumen

Entre los diversos métodos para mejorar la recuperación de petróleo de los yacimientos (estimulación de pozos), el uso de nanofluidos ha surgido como una alternativa prometedora para modificar la mojabilidad y permeabilidad de las rocas de arenisca. Por esta razón, en este estudio, se sintetizó óxido de grafeno (GO) a partir de grafito y se formuló un nanofluido utilizando GO disperso en agua para evaluar su capacidad para modificar la mojabilidad en núcleos de arenisca de yacimientos colombianos. El montaje experimental incluyó tres pruebas preliminares: mojabilidad visual, mediciones del ángulo de contacto y detergencia. Los resultados demostraron un aumento en la mojabilidad al agua de las rocas, lo que llevó a una disminución del ángulo de contacto del sistema agua-roca de hasta un 42.6%. Además, las pruebas de mojabilidad visual y detergencia arrojaron resultados positivos, indicando que el óxido de grafeno es un modificador efectivo de la mojabilidad, haciendo que la roca sea más mojada por agua.

**Palabras clave:** Modificador de Permeabilidad, Mojabilidad de Rocas, Óxido de Grafeno.

**Cómo citar:** Cárdenas, J.C., Pérez, A.S., Saez, R.T., León, E.A. (2023). Effect of Graphene Oxide Aqueous Dispersions on Rock Wettability. *Fuentes, el reventón energético*, 22 (1), 21-34. <https://doi.org/10.18273/revfue.v22n1-2024002> 

## **1. Introduction**

Improved Oil Recovery (IOR) in sandstone reservoirs is of great interest (Morrow & Buckley, 2011). Among the properties of sandstone reservoir rocks, wettability is the most critical parameter affecting the flow and distribution of fluids within the reservoir. In general, the efficiency of oil recovery hinges on rock wettability. In hydrophilic rocks, oil is primarily located in large pores within the rock matrix and exhibits high mobility under the influence of pressure differentials in the oil well. Conversely, in hydrophobic rocks, oil is confined to small pores and displays low mobility. Moreover, hydrophilic rocks possess higher water permeability compared to oil. Consequently, oil recovery from hydrophilic rocks surpasses that from hydrophobic rocks due to its elevated relative permeability (Wang et al., 2019; Bennett et al, 2004). Given that relative permeability is generally linked to rock wettability, one of the suggested mechanisms for enhancing oil recovery involves altering it to augment its water-wetting characteristics.

Additionally, significant challenges faced by wells producing oil and/or gas is formation damage. This refers to the loss of productivity resulting from the interaction of rocks with drilling and completion fluids (Chun et al., 1999). These fluids contain several polar surfactants and additives used to mitigate phenomena like invasion, corrosion, and emulsions, among others. Chemical additives can become adsorbed on the rock surface, leading to an alteration in wettability, and consequently, changes in relative permeability (González, 2014; Wang et al, 2013). These effects result in an increase in water/oil production ratios, negatively impacting the economic outcomes in the petroleum industry.

On the other hand, nanotechnology has recently emerged as an attractive technology in the Oil & Gas industry due to its exceptional characteristic that allows nanoparticles to flow through a porous medium without causing blockages or formation damage (Franco et al., 2017). Applications involving nanoparticles have been proposed as a promising technology that can be used synergistically with conventional treatments. Therefore, graphene and its derivatives, which are carbon-based nanomaterials

known for their mechanical resistance and flexibility, have garnered significant attention from the scientific community (Neuberger et al, 2018; Dreyer et al., 2010;). In the petroleum industry, these materials have gained popularity in recent years due to their applicability in various fields, including drilling fluids (Aftab et al., 2017; Yang et al., 2014b), lubricants (Berman et al., 2014b; Xu et al., 2011b), anticorrosive coatings (Singhbabu et al., 2015; Dumée et al., 2015), desalination (You et al., 2016), water/oil separation, and oil remediation (C. Liu et al., 2015; Liu et al., 2015; Hu et al., 2015), as well as emulsion stabilization (Zhang et al., 2014; McCoy et al., 2014; Kim et al., 2010), among others.

Graphene is a two-dimensional allotrope of carbon, defined structurally as a crystalline array formed by carbon atoms with sp<sup>2</sup> hybridization densely arranged in a hexagonal network, like a honeycomb (Terrones et al., 2010). Additionally, graphene oxide is the most representative derivative form produced through functionalization (oxidation) and exfoliation of graphite (Wei et al., 2014; Dikin et al., 2007). The oxidized structural form of graphene has not been entirely elucidated; however, during oxidation, a significant fraction of carbon atoms from graphite layers form new linkages with oxygen atoms. This results in the formation of different functional groups in the graphitic structure of exfoliated graphite: epoxides, hydroxyl, keto, and carboxylic groups (Figure 1) (Fang et al., 2016). Because of these modifications, graphene oxide is highly hydrophilic and hygroscopic. One of the key properties of GO is its wettability behavior. Previous reports have demonstrated that graphene is a neutral material with a contact angle for water ranging from 87 to 147°. However, GO exhibits hydrophilic properties with a contact angle with water of approximately 30-60° (Zhou & Xu 2020; Wei et al., 2014). For this reason, this material can be considered useful for applications involving wettability modification. Moreover, the presence of oxygenated groups and the planar two-dimensional structure confer surfactant properties to GO (Neto & Fileti, 2018; Kumar et al., 2017). These properties can alter the interfacial tension between oil and water phases. Additionally, GO presents an attractive opportunity for improving oil recovery due to the stability of its dispersion in brine with high salinity (Yoon et al., 2013).

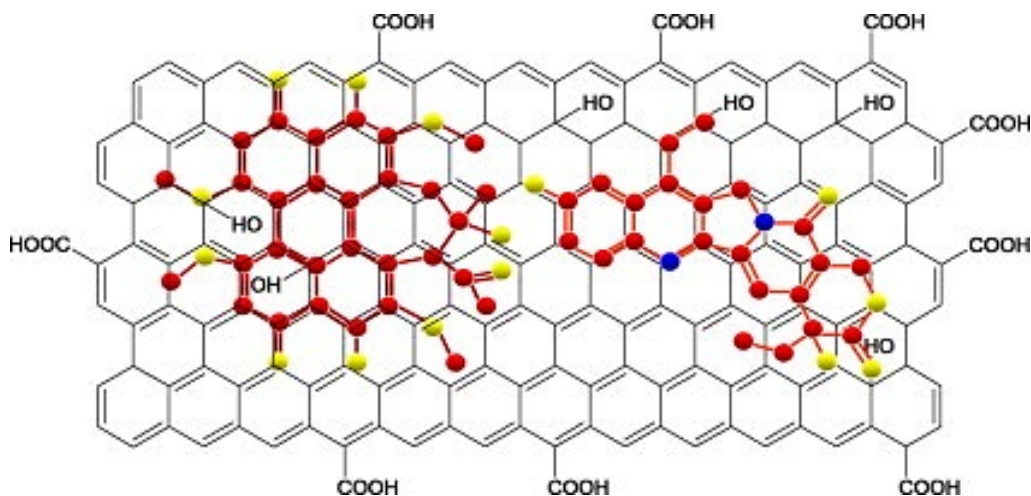


**Figure 1.** Probable Molecular Structure of Graphene Oxide (Zhou et al., 2014).

This work aims to study, at a laboratory scale, the use of a nanofluid based on graphene oxide as a modifier of rock wettability in order to improve oil recovery.

## 2. Experimental Section

### 2.1 Synthesis of Graphene Oxide Nanofluid

Graphene oxide synthesis was based in the Marcano et al. (2010) methodology with some modifications. The synthesis of Graphene Oxide (GO) was performed according to the following steps:

In an Erlenmeyer flask, 1 g of exfoliated graphite was combined with 133.4 mL of a solution containing  $H_2SO_4$  and  $H_3PO_4$  in a volumetric ratio of 9:1. Following this, 6 g of  $KMnO_4$  was slowly introduced while maintaining constant stirring at a low temperature of  $8^\circ C$ . Subsequently, the reaction temperature was raised to  $50^\circ C$  and left for 24 hours. Afterward, the reaction mixture was allowed to cool to room temperature.

Hydrogen peroxide (30% v/v) was then introduced into the cooled reaction mixture with agitation until the graphite was fully dispersed. The dispersed graphite oxide underwent hydrolysis with the addition of deionized water to the resulting yellow graphite oxide dispersion. The graphite oxide was subsequently decanted, and the solid material recovered through centrifugation at 500 rpm for 15 minutes. Following this, the graphite oxide sediment was subjected to an eight-fold washing process.

Graphite oxide was sonicated in a Sonics Ultrasonics processor VCX-750, utilizing a potency of 300W in pulsing mode. Afterward, six cycles of 15 minutes each were performed, resulting in a stable dispersion of graphene oxide. The solid graphene oxide was obtained by lyophilization at 0.140 mBar for a period of 72 hours from the GO liquid dispersion. This process was carried out using lyophilizer equipment (Labconco Freezone model 7754040).

### 2.2 Test of Wettability Modification

#### 2.2.1 Contact Angle Measurements

This test involves a qualitative evaluation of wettability (Vanegas, et al, 2016). and was conducted using rock samples from the Yariguí field. It begins by placing a liquid drop on the surface of the dry sample, followed by determining the contact angle for the liquid/air/fluid system using stereoscopy under atmospheric conditions.

Prior to treatment with the nanofluids to modify its wettability, the core material was pre-soaked with xylene to assess its initial wetness, which was confirmed through contact angle determinations using a HIROX KH7700 microscope. The subsequent step involved impregnating the oil-wet plugs with graphene oxide-based nanofluids at various concentrations. They were then dried, and their contact angles were re-evaluated. Additionally, this test was conducted by mixing graphene oxide with a commercially available sulfonated polyacrylamide to observe any changes in contact angles before and after nanofluid treatment.

## 2.2.2 Visual Wettability Tests

The visual wettability test was conducted to determine the impact of the treatment on the rock's wettability. Two types of samples were utilized: Ottawa sand and sandstone core material from the Yarigui oilfield. Ottawa sandstone naturally exhibits water-wetting characteristics. Consequently, this sample underwent a preliminary treatment with xylene to modify its wettability. Core samples from the Yarigui field did not require xylene treatment due to their inherent oil-wetting nature. To confirm the initial oil-wet state of both rock materials, a visual wettability test was performed using two cylindrical tubes, each containing 100 mL of brine (a hydrophilic solvent) or 100 mL of *varsol* (an organic solvent). Two grams of pulverized sandstone sample were added independently to each cylinder, and the aggregation or dispersion of sand particles was observed. Once the lipophilic behavior of the samples was confirmed (i.e., aggregation in brine or dispersion in *varsol*), the rock samples were treated with a 1,000 ppm GO-based nanofluid and left to impregnate for 1 hour under mild conditions. Subsequently, a visual wettability test was conducted to assess possible wettability modifications.

## 2.2.3 Detergency Tests

This test was performed using a reference Ottawa sandstone of 20/40 mesh. For this, ~5 g of sandstone was put in contact with 20 mL of GO-based nanofluid at a fixed concentration and mechanically stirred at atmospheric conditions. This dispersion was left by one hour, and then an excess of nanofluid was withdrawn, obtaining from this manner a nanofluid-impregnated sample. Then, 50 mL of brine was added to the impregnated sandstone and gently stirred and later heated by one hour at 85°C in an oven. After this, the treated sandstone samples, and their oil content was monitored.

## 3. Results and Discussion

### 3.1 Synthesis of GO-based Nanofluid

Synthesis of graphene oxide from graphite flakes is shown in Figure 2.

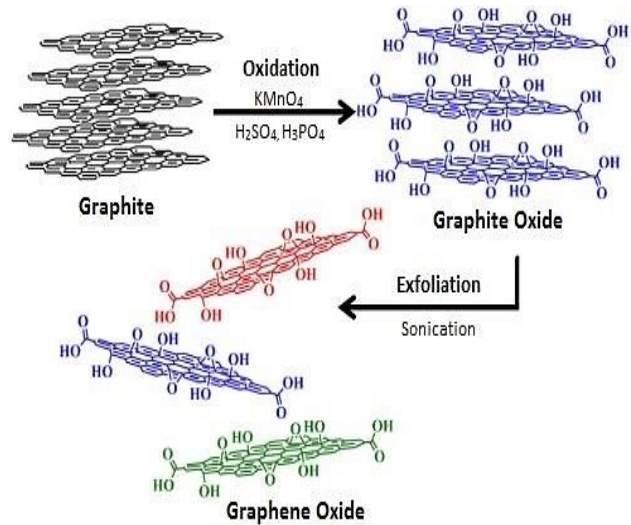


**Figure 2.** Comprehensive Diagram of Graphene Oxide Synthesis (Ammar et al., 2016).

In this reaction, graphite undergoes chemical oxidation and exfoliation. Graphite is composed of layers held together by van der Waals forces, forming a crystalline network of carbon atoms. The separation between layers is approximately 3.33 Å. Under acidic conditions, oxygenated groups such as hydroxyls, epoxides, and carboxylic acids attach to the graphite layers, increasing the interlayer distance to about 6.25 Å. This process also imparts a hydrophilic nature to these oxidized layers. Subsequently, they are exfoliated through ultrasonic treatment, resulting in the formation of graphene oxide (Gómez, 2012).

As depicted in Figure 3A, once graphite is oxidized, the color of this carbon material changes from black to purple. Simultaneously, Figure 3B shows an orange solution of graphite oxide due to the reduction of oxidizing agents and hydrolysis of graphite oxide. Furthermore, Figure 3C displays a brown mixture after sonication of graphite oxide for exfoliation, leading to the production of a graphene oxide aqueous dispersion. Lastly, the lyophilized product of the graphene oxide dispersion exhibits a foamy brown material (Figure 3D), characteristic of exfoliated graphene oxide.

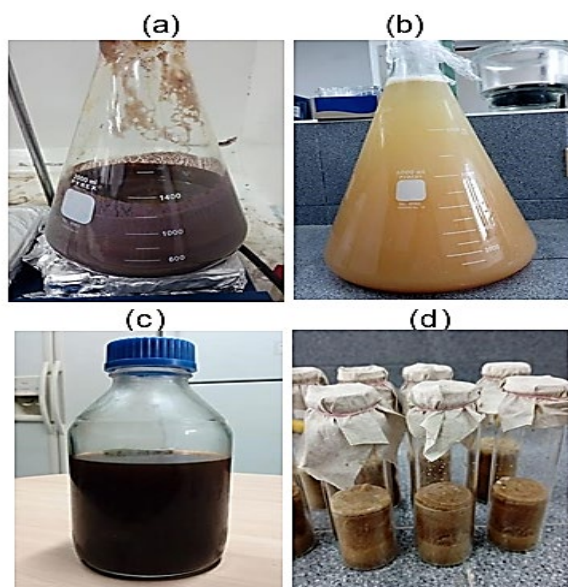


**Figure 3.** Experimental evidence of Graphene Oxide Synthesis (a) Graphite oxidation (b) Reduction of oxidizing agents and hydrolysis. (c) Water-dispersed graphene oxide (d) Solid graphene-oxide.

### 3.2 Physico-Chemical Characterization

Graphene oxide-based for the nanofluid formulation was characterized by FTIR, RAMAN, DLS, SEM, and EDS. this combination of techniques allows for a comprehensive characterization of the graphene oxide-based nanofluid, providing information about its chemical composition, molecular structure, particle size distribution, morphology, and elemental composition.

#### 3.2.1 UV-VIS Spectra

The UV-VIS spectrum of an aqueous dispersion of GO (See Figure 4A) exhibits a peak with maximum absorbance at 229 nm and a shoulder at 301 nm. These signals have been previously documented in the literature (Ammar et al., 2015; Marcano et al., 2010). The signal at 229 nm is attributed to the superposition of two electronic transitions: (i)  $\pi \rightarrow \pi^*$  transitions in C=C conjugated bonds from graphite, and (ii) the shoulder signal at 301 nm is attributed to  $n \rightarrow \pi^*$  transitions of C=O linkages. These features in the UV-Vis spectrum imply the presence of graphite material with oxidized functional groups.

#### 3.2.2 FTIR Analysis

To confirm the functionalization of graphite with oxygenated groups, FTIR analysis was conducted (Figure 4B). A stretching band corresponding to O-H bonds is observed at  $3,360 \text{ cm}^{-1}$  (Marcano et al., 2010; Geng et al., 2009; Guo et al., 2009; Wang et al., 2008). Simultaneously, bands at  $2,049$  and  $1,979 \text{ cm}^{-1}$  indicate C-H linkages (Guo et al., 2009), while bands at  $1,736$  and  $1,620 \text{ cm}^{-1}$  represent C=O and C=C bonds, respectively (Marcano et al., 2010; Guo et al., 2009; Si & Samulski, 2008). Additionally, stretching signals at  $1,416 \text{ cm}^{-1}$  for C-OH (Geng et al., 2009; Si & Samulski, 2008) were noted, and at  $1,224 \text{ cm}^{-1}$ , tension bonds for carboxylic acids (C-O) (Marcano et al., 2010; Si & Samulski, 2008) and epoxide groups (C-O-C) (Kumar et al., 2017; Dikin et al., 2007) were identified.

Finally, the stretching signal of C-O bonds from alcohols was detected at  $1,052 \text{ cm}^{-1}$  (Geng et al., 2009; Si & Samulski, 2008). The infrared analysis demonstrates that the bands obtained for the synthesized oxidized material from graphite contain functional groups commonly found in structural models of graphene oxide. This strongly indicates that the oxidation product is indeed graphene oxide.

#### 3.2.3 RAMAN

Figure 4C displays the Raman spectrum of the graphene oxide. Two prominent peaks at  $1,349$  and  $1,582 \text{ cm}^{-1}$ , corresponding respectively to the D and G bands, were observed. The D band originates from the stretching vibration of atoms in  $sp^3$  carbons, while the G band arises from the stretching vibration of  $sp^2$  carbons. Both are characteristic features of graphene oxide, as supported by the literature (Gómez, 2012; Marcano et al., 2010).

#### 3.2.4 DLS

The hydrodynamic size of the GO dispersion was determined using DLS. Figure 4D illustrates the relationship between particle number and particle size. A broad range of particle sizes, ranging from 60 to 500 nm, is evident. Approximately 90% of the particles measure 145 nm, with a mean size of 240 nm and a polydispersion index of 0.184.

### 3.2.5 SEM-EDX

In Figure 5A, SEM images of exfoliated graphene oxide are presented at 300x magnification. EDX analysis of chemical elements in the GO sample (Figure 5B) detected the presence of Carbon (C) and Oxygen (O), which are commonly found in graphene oxide. Additionally, residual manganese (Mn) and Sulfur (S) were observed, originating from the synthesis materials.

Furthermore, the thickness of graphene oxide layers is on a nanometric scale, rendering them highly flexible and imparting favorable properties for interaction with sandstone. This characteristic is also dependent on the size of the graphite used as a precursor. As a result, the synthesized GO should be suitable for modifying wettability and preventing potential pore plugging.

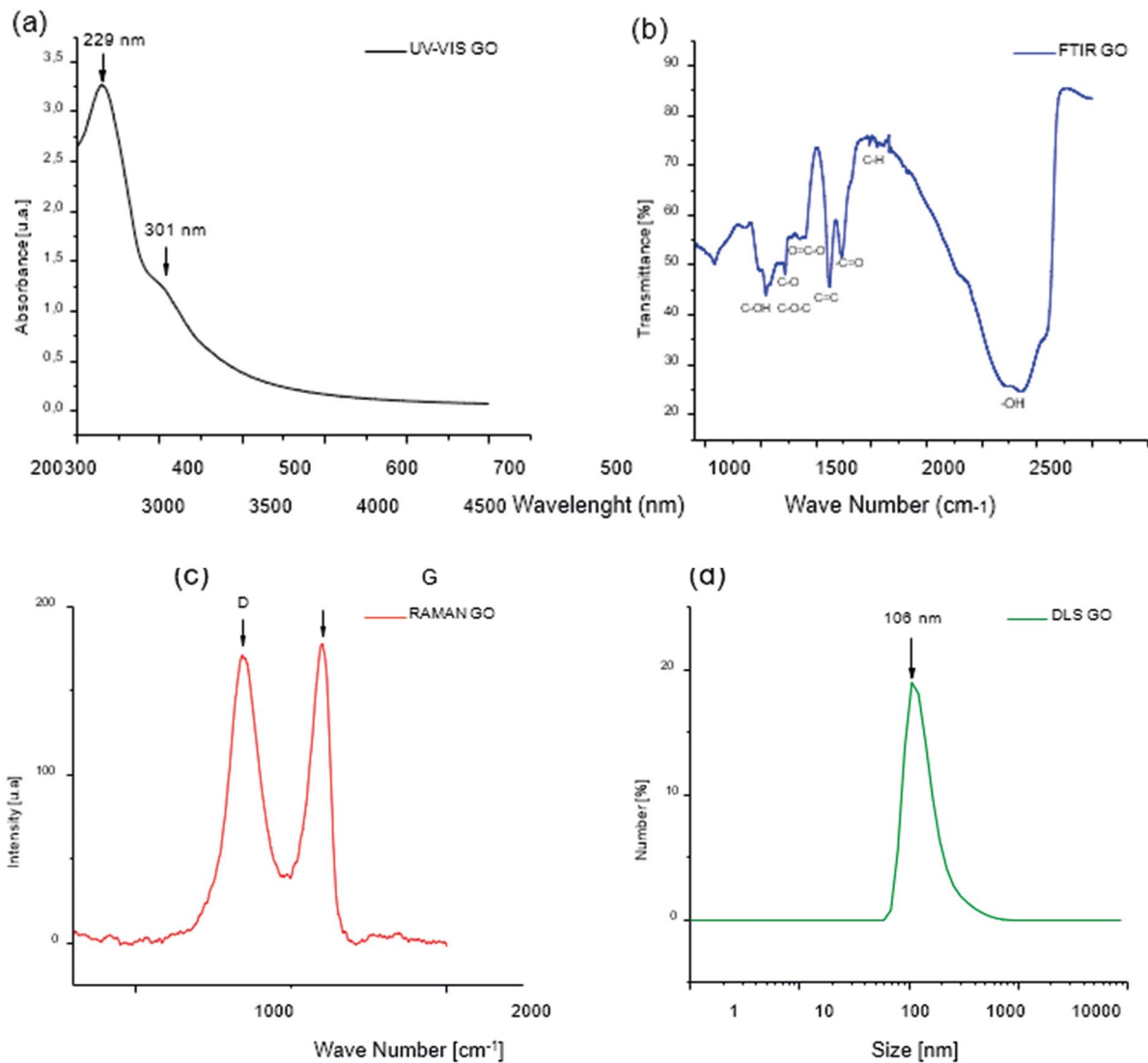
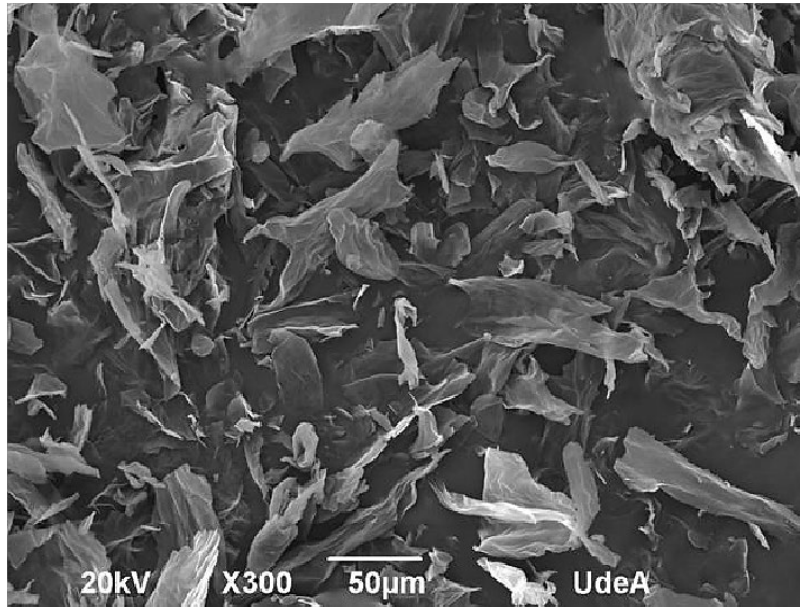


**Figure 4.** GO Spectra (A) UV-VIS. (B) FTIR (C) RAMAN (D) DLS.

(a)



(b)

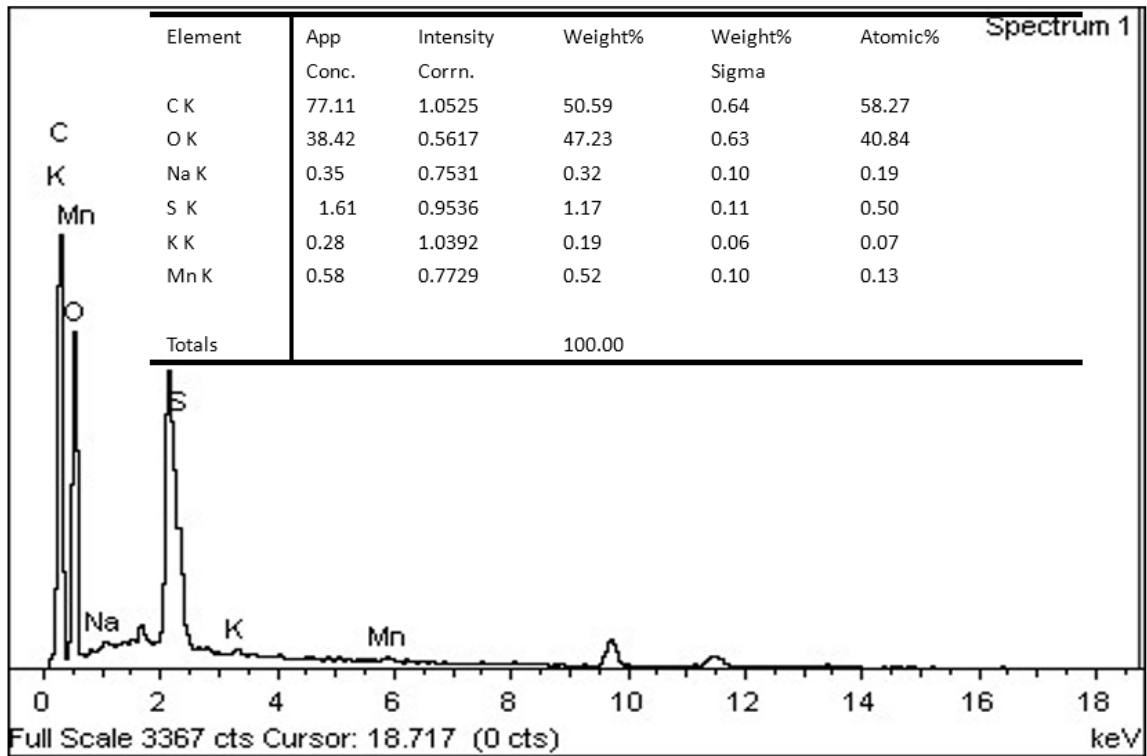
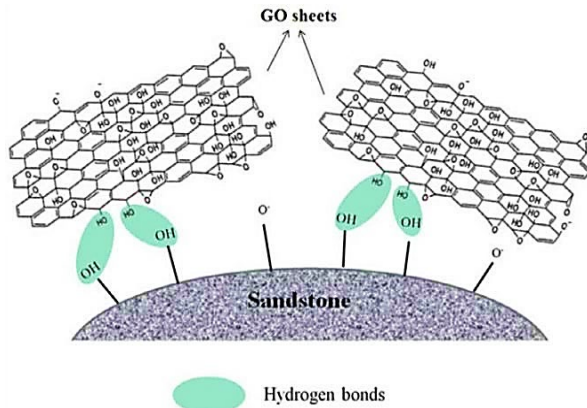


Figure 5. SEM X300 Image of Graphene Oxide (B)EDX spectrum.

### 3.3 Results of Wettability Tests

#### 3.3.1 Wettability by Contact Angle

The adsorption of graphene oxide onto rocks occurs through chemisorption. Previous studies (Radnia et al., 2017), have demonstrated that at low pH levels, adsorption is facilitated by hydrogen bonds between the oxygenated functional groups of GO layers and the hydroxyl groups on the silicon surfaces of sandstone rocks (Figure 6).



**Figure 6.** Interaction between graphene oxide and sandstone (Radnia et al., 2017).

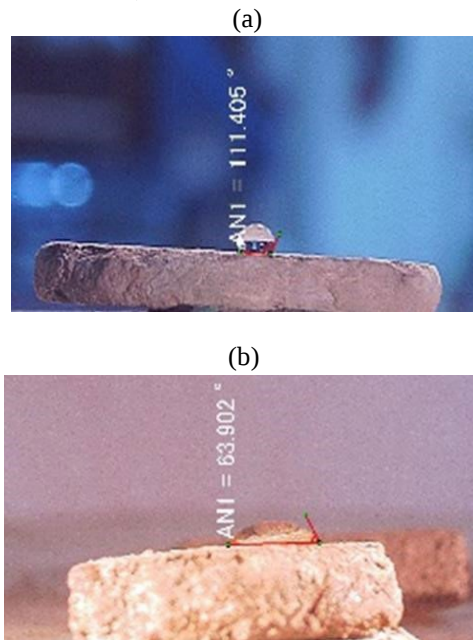


**Figure 7.** Image of water contact angles of sandstone rock treated with graphene oxide based-nanofluid (8,000ppm) (a) before treatment (b) after treatment.

Figure 7, depicts the effect of an 8,000 ppm graphene oxide-based nanofluid on water wettability, both before and after nanofluid treatment. The results of the effect of different concentrations of graphene oxide on water wettability are summarized in Table 1. It is observed that nanofluid treatments increased the wettability of sandstone rock to water. For example, 8,000 ppm of graphene oxide decreased the water contact angle by 42.6%, whereas at 500 ppm, it was only 27.1%. This indicates that GO can effectively alter rock wettability from oil-wet to water-wet and that this phenomenon is dependent on the concentration of GO. This is attributed to graphene oxide's richness in oxygenated groups (See Figure 1), which renders it a hydrophilic and hygroscopic material. Therefore, upon contact with water, water molecules interact with the pristine region of the GO through van der Waals forces. Simultaneously, electrostatic interaction plays a significant role in the oxidized region, forming a network of interfacial hydrogen bonds (Wei et al., 2014).

**Table 1.** Effect of nanofluid treatment on water wettability of sandstone rocks using different concentrations of graphene oxide based-nanofluids.

| NANOFLUID     | Contact Angle pre-treatment (°) | Contact Angle post-treatment (°) | Difference (%) |
|---------------|---------------------------------|----------------------------------|----------------|
| GO 8000 [ppm] | 111.4                           | 63.9                             | 42.6           |
| GO 5000 [ppm] | 110.3                           | 66.9                             | 39.3           |
| GO 3000 [ppm] | 120.9                           | 80.0                             | 33.7           |
| GO 1000 [ppm] | 105.9                           | 75.5                             | 28.7           |
| GO 500 [ppm]  | 101.4                           | 73.9                             | 27.1           |



On the other hand, the introduction of hydrophilic oxygenated functional groups into the graphene layers through oxidation increases the spacing between the GO membrane. Hence, water molecules can easily intercalate into the gaps between the functionalized graphite's intermediate layers (Liu et al., 2017) (See Figure 8), suggesting that this material can be utilized as an adsorbent for water molecules.

In addition to the electrostatic interactions between water and graphene oxide, the contact angle between water and graphene oxide decreases due to the corrugated morphology of GO layers after functionalization. Previous studies have revealed that GO layers are planar because their functionalization disrupts the  $sp^2$  hybridization nature of the C-C bond (Wei et al., 2014; Qiu et al., 2011). This corrugated conformation affects the wettability behavior of the GO because these wrinkles can act as capillary channels for the distribution of water throughout the GO structure (See Figure 9).

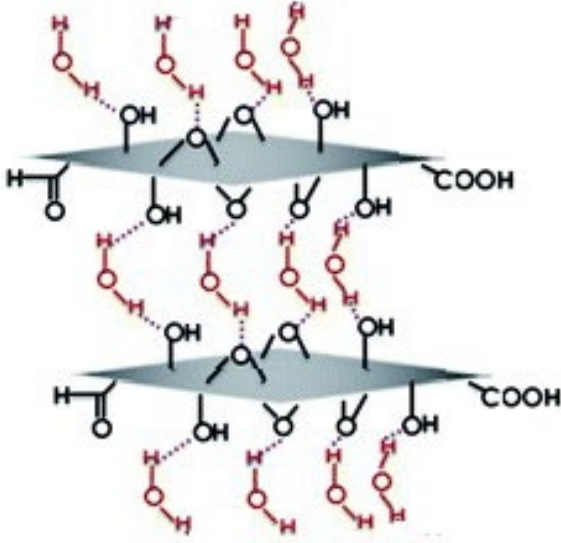


**Figure 8.** Intercalation of water molecules between graphene oxide layers (Liu et al., 2017).



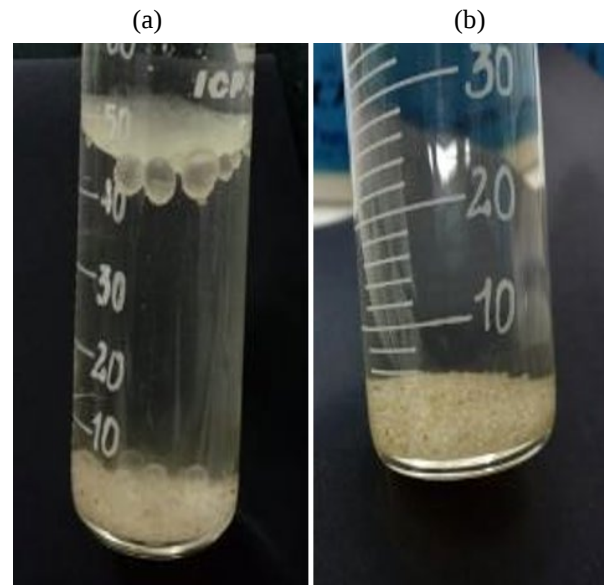
**Figure 9.** Diffusion of a water drop through corrugated layers from graphene oxide. (Nurrohman et al., 2023).

### 3.3.2 Visual Wettability

#### *Ottawa Sandstone.*

In Figure 10, images from visual wettability tests using Ottawa sandstone previously treated with xylene to enhance its oil-wettability are depicted. Prior to GO treatment, sandstone grains agglomerated, and no water dispersion was observed (Figure 10A). Conversely, no aggregation was observed when sandstone was introduced to varsol, and they dispersed easily (Figure 10B). However, after nanofluid treatment, sandstone grains were fully dispersed in water without aggregation (Figure 10C), while in varsol, they exhibited significant agglomeration (Figure 10D). The behavior of Ottawa sand grains treated with GO-based nanofluids suggests that GO altered the wettability of the grains from oil-wet to water-wet.

In this test, sandstone agglomeration occurs when grains come into contact with fluids of varying solvent properties. For example, when sand grains are coated with a hydrophobic material and then exposed to water, they are repelled and agglomerated in aqueous fluids. Similarly, if sand grains come into contact with graphene oxide, they undergo a wettability change, becoming hydrophilic and agglomerating when introduced to non-polar solvents like xylene.



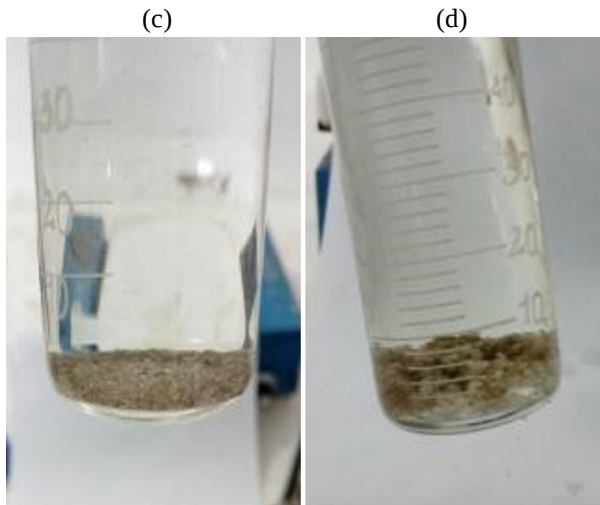


**Figure 10.** Images of visual wettability tests of Ottawa sand grains previously treated with xylene (A) in water before treatment with GO-based nanofluid; (B) in varsol before treatment with GO-based nanofluid; (C) in water after treatment with GO-based nanofluid, and (D) in varsol after treatment with GO-based nanofluid.

On the contrary, when sand grains are treated with a GO-based nanofluid, they disperse in aqueous fluids, engaging with water through hydrophilic interactions. As a result, sandstone grains previously soaked with xylene disperse in xylene. However, sand grains treated with GO-based nanofluids disperse in aqueous fluids without forming agglomerates.

In this scenario, the theoretical approach aligns with what was mentioned earlier regarding contact angles. The interaction between the oxygenated groups of graphene oxide and the silanol groups of sand enables adsorption onto the carbon material. Due to the compatibility and highly hydrophilic nature of sand covered with graphene oxide, it disperses seamlessly in water. In contrast, when introduced to a non-polar and hydrophobic liquid, it agglomerates.

### Core Plug Sections from Yarigui Oilfield

Figure 11, presents images from visual wettability tests conducted using sections of sandstone grain plugs obtained from the Yarigui Oilfield. These plugs were previously characterized and exhibited oil-wettability. Prior to treatment with graphene oxide-based nanofluids, sandstone grains did not disperse in water and instead agglomerated (Figure 11A). However, Figure 11B demonstrates the efficient dispersion of sandstone grains in varsol (a hydrophobic organic solvent).

In contrast, following the nanofluid treatment, sandstone grains were completely dispersed without any aggregation (Figure 11C), while in varsol, no dispersion was observed, and the grains agglomerated (Figure 11D). This indicates that graphene oxide altered the wettability of plug sections from the Yarigui Oilfield. This change in water wettability is likely attributed to the physicochemical properties of GO, which enhance the affinity of sandstone rocks to water.

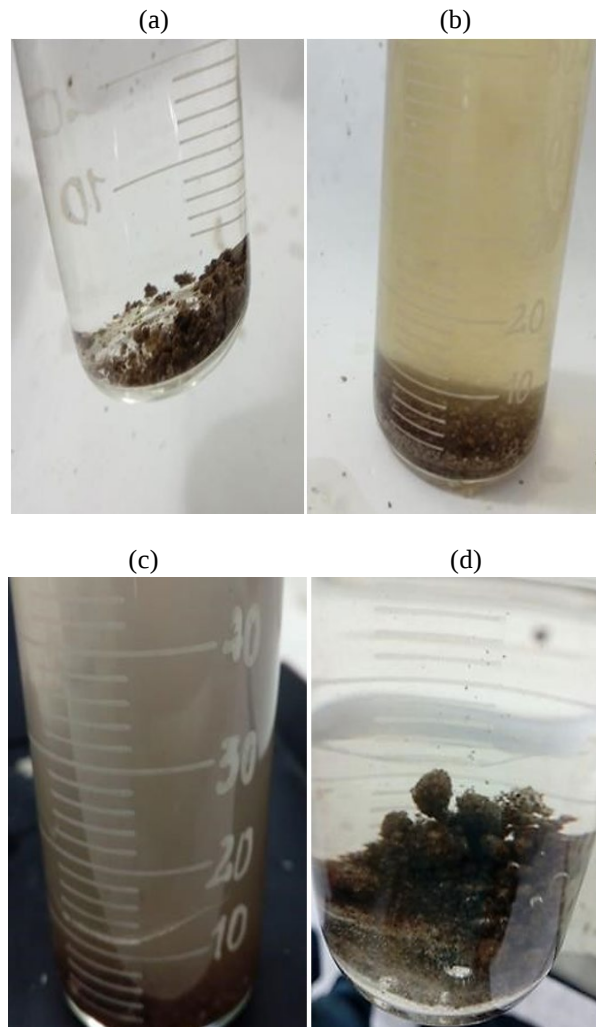


**Figure 11.** Images of visual wettability tests of Yarigui sandstone grains previously treated with xylene (A) in water before treatment with GO-based nanofluid; (B) in varsol before treatment with GO-based nanofluid; (C) in water after treatment with GO-based nanofluid; (D) in varsol after treatment with GO-based nanofluid.

### 3.3.3 Detergency

In Figure 12, the results of detergency tests using Ottawa sandstone (mesh 20/40) are presented. The sand grains were initially soaked with crude oil to ensure oil-wettability. Consequently, without nanofluid treatment, the sand grains remained impregnated with oil after one hour of stirring at 85°C, owing to the Ottawa sand's pronounced affinity for crude oil (Figure 12A).

In Figure 12B, two snapshots illustrate the detergency process of Ottawa sands treated with GO-based nanofluid. Graphene oxide primarily interacts with sandstone grains due to its highly hydrophilic nature, facilitating the cleaning process. As a result, sandstone grains treated with GO-based nanofluid were significantly cleaner under the treatment conditions. Put differently, graphene oxide displaced oleophilic fluids from the sandstone grains impregnated with GO. Consequently, this detergency effect indicates that graphene oxide exhibits similar behavior to surfactants, further demonstrating the alteration of sandstone wettability from its original oil-wettability.

The detergency test assesses the cleaning effectiveness of the surfactant dissolved in the treatment and indirectly measures the wettability it induces. If the surfactant possesses good detergency, the sand should be thoroughly cleaned. One of the most notable properties of graphene oxide is its surface activity. This property is characteristic of long-chain surfactants. However, the distribution of hydrophilic functional groups on the hydrophobic surface of graphene can confer amphiphilic properties to the functionalized system.

GO sheets exhibit amphiphilic characteristics with a distribution of hydrophilic and hydrophobic domains from the edge to the center. The presence of these domains on the GO surface influences its liquid-phase properties, particularly its interfacial activity. The results obtained in the detergency test, where the sand was practically cleaned, confirm the surfactant power (detergency) of graphene oxide, which indirectly measures its impact on water wettability, and thus, on the sand coated with this nanomaterial.

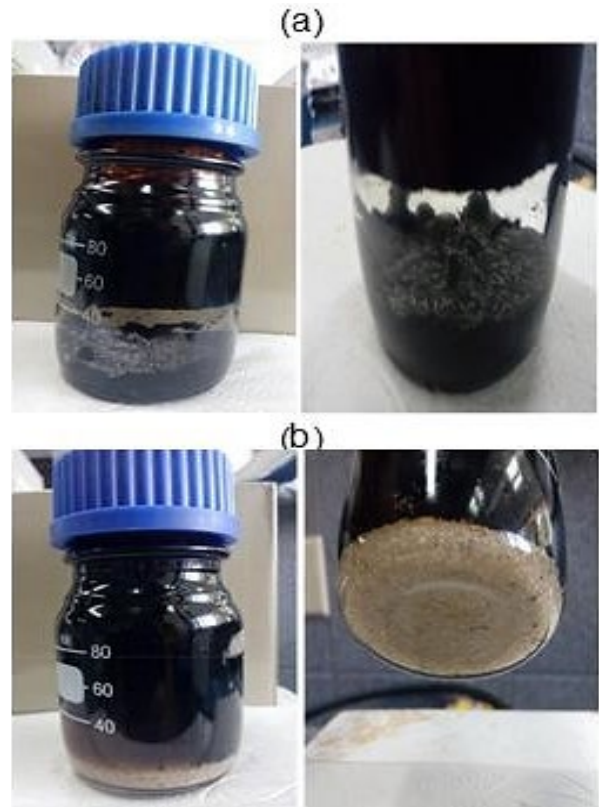


**Figure 12.** Images of detergency test with Ottawa sandstone previously impregnated with oil (A) No-treated with GO-based nanofluid (B) Treated with GO-based nanofluid.

### 4. Conclusions

- Graphene oxide was synthesized from graphite flakes and characterized through FTIR, RAMAN, and EDS analyses. SEM images revealed the exfoliation of graphene oxide into thin layers.
- The robust interaction between the oxygenated groups of graphene oxide and the silanol groups of the sand, combined with the hydrophilic properties conferred by graphene oxide to the sand previously coated with xylene, led to notable changes in water wettability in core sections obtained from sandstones of the Yarigui Oilfield treated with GO nanofluids. This was evidenced by a significant decrease in contact angle, with reductions of up to 42.6%. The variations in wettability were contingent on the concentrations of GO used in the nanofluid. For instance, with doses of 500 ppm GO, a 27% reduction in contact angle for water was achieved.

- Furthermore, following the same theoretical foundation of the wettability test, visual wettability tests demonstrated substantial improvements in water wettability for both sandstone samples.
- Finally, detergency tests highlighted the promising detergency properties of amphiphilic graphene oxide. Sandstones were nearly completely cleansed of oil after GO treatment.

## 5. Acknowledgments

Authors are thankful to the Colombian Petroleum Institute of Ecopetrol S.A and the Universidad Industrial de Santander for their unconditional support for the completion of this work.

## References

- [1] Aftab, A., Ismail, A. R., & Ibupoto, Z. H. (2017). Enhancing the rheological properties and shale inhibition behavior of water-based mud using nanosilica, multi-walled carbon nanotube, and graphene nanoplatelet. *Egyptian Journal of Petroleum*, 26(2), 291–299. <https://doi.org/10.1016/j.ejpe.2016.05.004>
- [2] Ammar, A., Al-Enizi, A. M., Al-Maadeed, M., & Karim, A. (2016). Influence of graphene oxide on mechanical, morphological, barrier, and electrical properties of polymer membranes. *Arabian Journal of Chemistry*, 9(2), 274–286. <https://doi.org/10.1016/j.arabjc.2015.07.006>
- [3] Bennett, B., Buckman, J.O., Bowler, B., & Larter, S. R. (2004). Wettability alteration in petroleum systems: the role of polar non-hydrocarbons. *Petroleum Geoscience*, 10(3), 271–277. <https://doi.org/10.1144/1354-079303-606>
- [4] Berman, D., Erdemir, A., & Sumant, A. V. (2014). Graphene: a new emerging lubricant. *Materials Today*, 17(1), 31–42. <https://doi.org/10.1016/j.mattod.2013.12.003>
- [5] Chun, H., Zhiqiang, T., & Guancheng, J. (1999). Effect of wettability on water injection recovery factor of heavy oil reservoir of Kendong Block 29. *Oil Drilling & Production Technology*, 21(3), 92–94.
- [6] Dikin, D. A., Stankovich, S., Zimney, E. J., Piner, R. D., Dommett, G., Evmenenko, G., Nguyen, S. T., & Ruoff, R. S. (2007). Preparation and characterization of graphene oxide paper. *Nature*, 448, 457–460. <https://doi.org/10.1038/nature06016>
- [7] Dreyer, D. R., Park, S., Bielawski, C. W., & Ruoff, R. S. (2010). The chemistry of graphene oxide. *Chemical Society Reviews*, 39(1), 228–240. <https://doi.org/10.1039/b917103g>
- [8] Dumée, L. F., He, L., Wang, Z., Sheath, P., Xiong, J., Feng, C., Tan, M.Y., She, F., Duke, M., Gray, S., Pacheco, A., Hodgson, P., Majumder, M., & Kong, L. (2015). Growth of nano-textured graphene coatings across highly porous stainless steel supports towards corrosion resistant coatings. *Carbon*, 87, 395–408. <https://doi.org/10.1016/j.carbon.2015.02.042>
- [9] Espinoza, J. M. (2014). Daño a la formación en pozos petroleros, Bachelor's thesis, *Universidad Nacional Autónoma de México*. <https://hdl.handle.net/20.500.14330/TES01000715173>
- [10] Fang, S., Chen, T., Wang, R., Xiong, Y., Chen, B., & Duan, M. (2016). Assembly of Graphene Oxide at the Crude Oil/Water Interface: A New Approach to Efficient Demulsification. *Energy & Fuels*, 30(4), 3355–3364. <https://doi.org/10.1021/acs.energyfuels.6b00195>
- [11] Franco, C. A., Zabala, R. D., & Cortés, F. B. (2017). Nanotechnology applied to the enhancement of oil and gas productivity and recovery of Colombian fields. *Journal of Petroleum Science and Engineering*, 157, 39–55. <https://doi.org/10.1016/j.petrol.2017.07.004>
- [12] Geng, Y., Wang, S. J., & Kim, J-K. (2009). Preparation of graphite nanoplatelets and graphene sheets. *Journal of Colloid and Interface Science*, 336(2), 592–598. <https://doi.org/10.1016/j.jcis.2009.04.005>
- [13] Gómez, I. (2012). Síntesis y caracterización de grafeno químicamente reducido, empleando técnicas espectroscópicas y microscopía electrónica de barrido, Bachelor's tesis - *Universidad Industrial de Santander*.

- [14] Guo, H-L., Wang, X-F., Qian, Q-Y., Wang, F.-B., & Xia, X-H. (2009). A Green Approach to the Synthesis of Graphene Nanosheets. *ACS Nano*, 3(9), 2653–2659. <https://doi.org/10.1021/nn900227d>
- [15] Hu, X., Yu, Y., Zhou, J., Wang, Y., Liang, J., Zhang, X., Chang, Q., & Song, L. (2015). The improved oil/water separation performance of graphene oxide modified Al<sub>2</sub>O<sub>3</sub> microfiltration membrane. *Journal of Membrane Science*, 476, 200–204. <https://doi.org/10.1016/j.memsci.2014.11.043>
- [16] Kim, J., Cote, L. J., Kim, F., Yuan, W., Shull, K. R., & Huang, J. (2010). Graphene Oxide Sheets at Interfaces. *Journal of the American Chemical Society*, 132(23), 8180–8186. <https://doi.org/10.1021/ja102777p>
- [17] Kumar, H.V., Huang, K. Y-S., Ward, S. P., & Adamson, D. H. (2017). Altering and investigating the surfactant properties of graphene oxide. *Journal of Colloid and Interface Science*, 493, 365–370. <https://doi.org/10.1016/j.jcis.2017.01.043>
- [18] Liu, R., Gong, T., Zhang, K., & Lee, C. (2017). Graphene oxide papers with high water adsorption capacity for air dehumidification. *Scientific Reports*, 7(1). <https://doi.org/10.1038/s41598-017-09777-y>
- [19] Liu, C., Yang, J., Tang, Y., Yin, L., Tang, H., & Li, C. (2015). Versatile fabrication of the magnetic polymer-based graphene foam and applications for oil–water separation. *Colloids and Surfaces A: Physicochemical and Engineering Aspects*, 468, 10–16. <https://doi.org/10.1016/j.colsurfa.2014.12.005>
- [20] Liu, Y., Zhou, J., Zhu, E., Tang, J., Liu, X., & Tang, W. (2015). Covalently intercalated graphene oxide for oil–water separation. *Carbon*, 82, 264–272. <https://doi.org/10.1016/j.carbon.2014.10.070>
- [21] Marcano, D. C., Kosynkin, D. V., Berlin, J. M., Sinitskii, A., Sun, Z., Slesarev, A., Alemany, L. B., Lu, W., & Tour, J. M. (2010). Improved Synthesis of Graphene Oxide. *ACS Nano*, 4(8), 4806–4814. <https://doi.org/10.1021/nn1006368>
- [22] McCoy, T. M., Pottage, M. J., & Tabor, R. F. (2014). Graphene Oxide-Stabilized Oil-in-Water Emulsions: pH-Controlled Dispersion and Flocculation. *The Journal of Physical Chemistry C*, 118(8), 4529–4535. <https://doi.org/10.1021/jp500072a>
- [23] Morrow, N., & Buckley, J. (2011). Improved Oil Recovery by Low-Salinity Waterflooding. *Journal of Petroleum Technology*, 63(05), 106–112. <https://doi.org/10.2118/129421-jpt>
- [24] Neto, A., & Fileti, E. E. (2018). Elucidating the amphiphilic character of graphene oxide. *Physical Chemistry Chemical Physics*, 20(14), 9507–9515. <https://doi.org/10.1039/c8cp00797g>
- [25] Neuberger, N., Adidharma, H., & Fan, M. (2018). Graphene: A review of applications in the petroleum industry. *Journal of Petroleum Science and Engineering*, 167, 152–159. <https://doi.org/10.1016/j.petrol.2018.04.016>
- [26] Nurrohman, N., Almisbahi, H., Albeirutty, M., Bamaga, O., Almatrafi, E., Tocci, E. (2023). Graphene coating reduces the heat transfer performance of water vapor condensation on copper surfaces: A molecular simulation study. *Alexandria Engineering Journal*, 82, 101-125. <https://doi.org/10.1016/j.aej.2023.09.076>
- [27] Qiu, L., Zhang, X., Yang, W., Wang, Y., Simon, G. P., & Li, D. (2011). Controllable corrugation of chemically converted graphene sheets in water and potential application for nanofiltration. *Chemical Communications*, 47(20), 5810-5812. <https://doi.org/10.1039/c1cc10720h>
- [28] Radnia, H., Nazar, A., & Rashidi, A. (2017). Experimental assessment of graphene oxide adsorption onto sandstone reservoir rocks through response surface methodology. *Journal of the Taiwan Institute of Chemical Engineers*, 80, 34–45. <https://doi.org/10.1016/j.jtice.2017.07.033>
- [29] Si, Y., & Samulski, E. T. (2008). Synthesis of Water Soluble Graphene. *Nano Letters*, 8(6), 1679–1682. <https://doi.org/10.1021/nl080604h>

- [30] Singhbabu, Y. N., Sivakumar, B., Singh, J. K., Bapari, H., Pramanick, A. K., & Sahu, R. K. (2015). Efficient anti-corrosive coating of cold-rolled steel in a seawater environment using an oil-based graphene oxide ink. *Nanoscale*, 7(17), 8035–8047. <https://doi.org/10.1039/c5nr01453k>
- [31] Terrones, M., Botello-Méndez, A. R., Campos-Delgado, J., López-Urías, F., Vega-Cantú, Y. I., Rodríguez-Macías, F. J., Elías, A. L., Muñoz-Sandoval, E., Cano-Márquez, A. G., Charlier, J. C., & Terrones, H. (2010). Graphene and graphite nanoribbons: Morphology, properties, synthesis, defects and applications. *Nano Today*, 5(4), 351–372. <https://doi.org/10.1016/j.nantod.2010.06.010>
- [32] Vanegas, C. L., Buendia, H., & Carrillo, L. F. (2016). Evaluación y selección de un inhibidor multiscala para prevenir la formación de incrustaciones inorgánicas en un campo petrolero colombiano. *Fuentes, el reventón energético*, 14(2), 111-120. <https://revistas.uis.edu.co/index.php/revistafuentes/article/view/6075>
- [33] Wang, Y-L., Ma, L., Bai, B-J., Jiang, G., Jin, J-F., & Wang, Z-B. (2013). Wettability Alteration of Sandstone by Chemical Treatments. *Journal of Chemistry*, 1–8. <https://doi.org/10.1155/2013/845031>
- [34] Wang, D., Sun, S., Cui, K., Li, H., Gong, Y., Hou, J., & Zhang, Z. (2019). Wettability Alteration in Low-Permeability Sandstone Reservoirs by “SiO<sub>2</sub>-Rhamnolipid” Nanofluid. *Energy & Fuels*, 33(12), 12170–12181. <https://doi.org/10.1021/acs.energyfuels.9b01930>
- [35] Wang, G., Yang, J., Park, J., Gou, X., Wang, B., Liu, H., & Yao, J. (2008). Facile Synthesis and Characterization of Graphene Nanosheets. *The Journal of Physical Chemistry C*, 112(22), 8192–8195. <https://doi.org/10.1021/jp710931h>
- [36] Wei, N., Lv, C., & Xu, Z. (2014). Wetting of Graphene Oxide: A Molecular Dynamics Study. *Langmuir*, 30(12), 3572–3578. <https://doi.org/10.1021/la500513x>
- [37] Xu, L., Ma, T-B., Hu, Y-Z., & Wang, H. (2011). Vanishing stick-slip friction in few-layer graphenes: the thickness effect. *Nanotechnology*, 22(28), 285708. <https://doi.org/10.1088/0957-4484/22/28/285708>
- [38] Xuan, Y., Jiang, G., & Li, Y. (2014). Nanographite Oxide as Ultrastrong Fluid-Loss-Control Additive in Water-Based Drilling Fluids. *Journal of Dispersion Science and Technology*, 35(10), 1386–1392. <https://doi.org/10.1080/01932691.2013.858350>
- [39] Yoon, K. Y., An, S. J., Chen, Y., Lee, J. H., Bryant, S. L., Ruoff, R. S., Huh, C., & Johnston, K. P. (2013). Graphene oxide nanoplatelet dispersions in concentrated NaCl and stabilization of oil/water emulsions. *Journal of Colloid and Interface Science*, 403, 1–6. <https://doi.org/10.1016/j.jcis.2013.03.012>
- [40] You, Y., Sahajwalla, V., Yoshimura, M., & Joshi, R. (2016). Graphene and graphene oxide for desalination. *Nanoscale*, 8(1), 117–119. <https://doi.org/10.1039/c5nr06154g>
- [41] Zhang, L., Shi, T., Tan, D., Zhou, H., & Zhou, X. (2014). Pickering Emulsion Polymerization of Styrene Stabilized by the Mixed Particles of Graphene Oxide and NaCl. *Fullerenes Nanotubes and Carbon Nanostructures*, 22(8), 726–737. <https://doi.org/10.1080/1536383x.2012.731581>
- [42] Zhou, K., & Xu, Z. (2020). Ion Permeability and Selectivity in Composite Nanochannels: Engineering through the End Effects. *Journal of Physical Chemistry C*, 124(8), 4890–4898. <https://doi.org/10.1021/acs.jpcc.9b11750>
- [43] Zhou, L., Zhou, L., Wei, Z., Ge, X., Zhou, J., Jiang, H., Li, F., Shen, J. (2014). Combination of chemotherapy and photodynamic therapy using graphene oxide as drug delivery system. *Journal of Photochemistry and Photobiology B: Biology*, 135, 7-16. <https://doi.org/10.1016/j.jphotobiol.2014.04.010>